Vol 13 No 12, December 2004
1009-1963/2004/13(12)/1982-10

Chinese Physics

© 2004 Chin. Phys. Soc.
and IOP Publishing Ltd

Effects of interface kinetics and anisotropy on the stability of the growing crystal face and dissolution face during crystallization from solution under microgravity

Zhu Zhen-He(朱振和)[a)b)], Hong Yong(洪 勇)[a)c)],
Ge Pei-Wen(葛培文)[a)], and Yu Yu-De(俞育德)[a)]

[a)] *Institute of Physics, Chinese Academy of Sciences, Beijing* 100080, *China*
[b)] *Department of Physics, Central University for Nationalities, Beijing* 100081, *China*
[c)] *Department of Chemistry, University of Science and Technology of Beijing, Beijing* 100083, *China*

(Received 7 September 2003; revised manuscript received 13 July 2004)

The stability of the shapes of the growing crystal face and dissolution face in a two-dimensional mathematical model of crystal growth from solution under microgravity is studied. Effects of the interface kinetics and anisotropy of crystallization and dissolution on the stability are also studied. It is proved that the stable shapes of crystal growth face and dissolution face do exist, which are of suitably shaped curves with their upper parts inclined backward properly no matter whether the interface kinetics and the anisotropy are taken into account or not. The stable shapes of the growing crystal faces and dissolution faces are calculated for various cases. The interface kinetics will make the inclination degree of stable crystal growth face reduce and that of stable dissolution face reduce slightly. The anisotropy of crystallization and dissolution may make the inclination degree of stable-growing crystal face smaller or larger, and that of the stable dissolution face varies very slightly.

Keywords: microgravity conditions, growth from solution, interface, interface kinetics, crystallization anisotropy
PACC: 0260, 0540, 8110D

1. Introduction

Extensive studies on crystal growth in space have been performed recently. In a series of our previous papers,[1−12] the characteristics of crystal growth from solution under microgravity were analysed in detail with a cuboidal container model by computing the steady-state solutions of certain sets of partial differential equations. It is reasonable to do this only when the crystal growth rate is very slow and quasi-steady conditions are satisfied. The quasi-steady conditions include the requirement that the geometrical shape of the model should not change during the crystal growth. Using this model, the spatial distribution of the solute concentration, that of the temperature and fluid velocity, the streamline graph and the crystal growth rate can be calculated. The fluid convection and the solute diffusion have been studied. Our calculations show that, in general, the convection plays a dominant role in the solute transport.[1−3] At the same time, the effects of various physical and geometrical parameters, the orientation of microgravity, the boundary condition, the seed crystal dimensions and the interface kinetics of crystallization and dissolution on the characteristics of the crystal growth from solution have also been studied.[3−5,8,10−12] We have obtained some scaling laws in certain regions of parameter (the Rayleigh number Ra, the Prandtl number Pr, the Schmidt number Sc) space.[6−8,10] The influences of the fluctuations of the gravity level and the temperature at the growth face of the crystal on the crystal growth from solution have been studied.[9,11] However, the stability of the growing crystal face and the dissolution face was left out of the account in Refs.[1–12].

In the cuboidal container model, the dimension of the container in the z-direction is long enough to sim-

plify the mathematical problem as a two-dimensional (2D) problem, and the edges of the container which constitute the x-axis and y-axis are a and b in length, respectively, i.e. $0 \leq x \leq a$ and $0 \leq y \leq b$. The growth face of seed crystal is the plane of $x = 0$ and the dissolution face of the crystal of solute source is the plane of $x = a$. It has been shown by calculation that the crystal growth rates are functions of y under all kinds of conditions.[1,3,5,13,14] This means that the shape of the crystal growth face will change during crystal growth. This is, however, inconsistent with the supposition of quasi-steady state. Therefore, the stable growing crystal face must not be the plane of $x = 0$ if it can exist. We have proven that when the crystal starts growing from the plane face of $x = 0$, the upper part of the crystal growth face is going to incline forward and the inclination gets greater and greater.[15,16] This result has been verified in an experiment of ice growth.[17] We have also proven that the stable growing crystal face does exist and have calculated its stable shapes for various values of parameters, Ra, Pr and Sc.[15,16]

For the same reason, the dissolution face of plane $x = a$ is unstable and its shape will also change during the dissolution of the source crystal. We have proven that a stable dissolution face does exist and have calculated its stable shapes for various values of parameters, Pa, Pr, and Sc.[18]

In Refs.[15,16,18], only the effects of the convection diffusion in the solution have been taken into account; the effects of the interface kinetics and the anisotropy of crystallization and dissolution have been left unaccounted for. We study the effects of the interface kinetics and the anisotropy of crystallization and dissolution on the stable shapes of the growing crystal face and dissolution face in this paper.

2. Model

The model employed here is similar to that used in Refs.[18], which is a container filled with the parent solution. A curved face expressed by $x = f(y)$ and $f(0) = 0$ and another curved face expressed by $x = f_i(y)$ and $f_i(0) = a$ are the crystal growth face and the surface of the container wall made of the material of solute source, respectively. The surface of the top and bottom walls of the container are the planes of $y = b$ and $y = 0$, respectively. The bottom edge of the container in the x-direction is a in length. The dimension of the container in the z-direction is assumed to be long enough to simplify the mathematical problem as a 2D problem. The orientation of gravity is along the -y direction.

The temperatures at the crystal growth face and the dissolution face are kept as T_s and T_i, respectively. The equilibrium solubilities at temperatures of T_s and T_i are c_s and c_i, respectively. The solution in contact with a growing crystal face is supersaturated and the supersaturation distribution is not uniform.[19] Supersaturation is the driving force for crystal growth. The solution in contact with a source crystal face is undersaturated and the undersaturation distribution is also not uniform.[19] Undersaturation is the driving force for dissolution. When the interface kinetics is taken into account, the boundary condition of Eq.(24) of Ref.[18] becomes[10,20]

$$\left.\frac{\partial\phi(X,Y)}{\partial n}\right|_{X=f(Y)} = K(\phi - 1),$$

$$\left.\frac{\partial\phi(X,Y)}{\partial n}\right|_{X=f_i(Y)} = -K'\phi, \qquad (1)$$

where K and K' are the dimensionless interface kinetics coefficients,[10,20] $K = ka/D$ and $K' = k'a/D$ (D is the solute diffusion coefficient), k is the interface kinetics coefficient for crystallization and k' is that for dissolution. The temperatures at the surface of the top and bottom walls are taken to be two linear functions of x,

$$T(x,b) = T_s + (T_i - T_s)[x - f(b)]/[f_i(b) - f(b)] \quad (2)$$

and

$$T(x,0) = T_s + (T_i - T_s)x/a, \qquad (3)$$

respectively.

Figure 1 illustrates the model used in this paper and the Cartesian coordinate system for it. It is known from our previous calculations[1−6] that all the calculation results for the case that the variation of solution density caused by temperature change is greater than that caused by solute concentration change are similar to those for the case that the variation of solution density caused by the solute concentration change is greater than that caused by the temperature change. The only difference is that the solution flows counterclockwise in the former case and clockwise in the latter case. If the physical parameters for aqueous solution are taken, it can be shown by calculation[6] that the variation of solution density caused by solute concentration change can be omitted and only that caused by the temperature change needs to be taken into account; the error caused by the omission is less than

1%. So, this approximation has been taken in most of our previous papers. It will be also adopted in this paper.

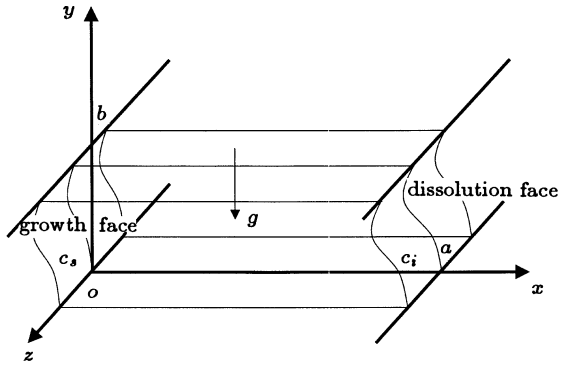


Fig.1. Coordinate system for the model used in the text.

3. Equations of motion

The dimensionless equations of motion are the same as Eqs.(3)–(6) of Ref.[18], and expressed as

$$\nabla_R^2 \Xi = \frac{1}{Pr}\left(\frac{\partial \Psi}{\partial Y}\frac{\partial \Xi}{\partial X} - \frac{\partial \Psi}{\partial X}\frac{\partial \Xi}{\partial Y}\right) - Ra\frac{\partial \theta}{\partial X}, \quad (4)$$

$$\nabla_R^2 \theta = \frac{\partial \Psi}{\partial Y}\frac{\partial \theta}{\partial X} - \frac{\partial \Psi}{\partial X}\frac{\partial \theta}{\partial Y}, \quad (5)$$

$$\nabla_R^2 \Psi = \Xi, \quad (6)$$

$$\nabla_R^2 \phi = \frac{Sc}{Pr}\left(\frac{\partial \Psi}{\partial Y}\frac{\partial \phi}{\partial X} - \frac{\partial \Psi}{\partial X}\frac{\partial \phi}{\partial Y}\right), \quad (7)$$

where the operator ∇_R^2 is defined as

$$\nabla_R^2 = \frac{\partial^2}{\partial X^2} + \frac{\partial^2}{\partial Y^2}, \quad (8)$$

λ is a dimensionless parameter given by

$$\lambda = b/a, \quad (9)$$

X, Y, $\boldsymbol{V}$ are dimensionless variables given by

$$X = x/a, \quad Y = y/a, \quad (10)$$

$$\boldsymbol{V} = (a/\chi)\boldsymbol{v}, \quad (11)$$

where $\boldsymbol{v}$ is the fluid velocity, χ is the thermal diffusion coefficient, Ψ, Ξ, ϕ, θ are dimensionless functions given by

$$\Psi = (1/\chi)\psi, \quad \Xi = (a^2/\chi)\xi, \quad (12)$$

$$\phi = (c_i - c)/(c_i - c_s), \quad (13)$$

$$\theta = (T_i - T)/(T_i - T_s). \quad (14)$$

The Rayleigh number Ra, the Prandtl number Pr and the Schmidt number Sc are defined as follows:

$$Ra = a^3\beta g_0 g(T_i - T_s)/(\nu\chi), \quad (15)$$

$$Pr = \nu/\chi, \quad (16)$$

$$Sc = \nu/D, \quad (17)$$

where ν is the kinematic viscosity, D is the solute diffusion coefficient, g_0 is the terrestrial acceleration of gravity, g is the gravity level and β is the thermal expansion coefficient which is given by

$$\beta = -\frac{1}{\rho_0}\left(\frac{\partial \rho}{\partial T}\right)_0, \quad (18)$$

where

$$\rho_0 = \rho(c_0, T_0). \quad (19)$$

The boundary conditions associated with Eqs.(4)–(7) are similar to those in Ref.[18]. They are expressed as

$$\left.\frac{\partial \Psi(X,Y)}{\partial X}\right|_{X=f(Y)} = \left.\frac{\partial \Psi(X,Y)}{\partial Y}\right|_{X=f(Y)} = \left.\frac{\partial \Psi(X,Y)}{\partial X}\right|_{X=f_i(Y)} = \left.\frac{\partial \Psi(X,Y)}{\partial Y}\right|_{X=f_i(Y)} = 0, \quad (20)$$

$$\frac{\partial \Psi(X,0)}{\partial X} = \frac{\partial \Psi(X,\lambda)}{\partial X} = \left.\frac{\partial \Psi(X,Y)}{\partial Y}\right|_{Y=0} = \left.\frac{\partial \Psi(X,Y)}{\partial Y}\right|_{Y=\lambda} = 0, \quad (21)$$

$$\Psi(X,Y)|_{X=f(Y)} = \Psi(X,Y)|_{X=f_i(Y)} = \Psi(X,0) = \Psi(X,\lambda) = 0, \quad (22)$$

$$\theta(X,Y)|_{X=f(Y)} = 1, \qquad \theta(X,Y)|_{X=f_i(Y)} = 0, \quad (23)$$

$$\theta(X,0) = 1 - X, \qquad \theta(X,\lambda) = 1 - \frac{X - f(\lambda)}{f_i(\lambda) - f(\lambda)}, \quad (24)$$

$$\left.\frac{\partial \phi(X,Y)}{\partial Y}\right|_{Y=0} = \left.\frac{\partial \phi(X,Y)}{\partial Y}\right|_{Y=\lambda} = 0, \quad (25)$$

$$\left.\frac{\partial \phi}{\partial X}\right|_{X=f(Y)} \frac{1}{\sqrt{1+[f'(Y)]^2}} - \left.\frac{\partial \phi}{\partial Y}\right|_{X=f(Y)} \frac{f'(Y)}{\sqrt{1+[f'(Y)]^2}} = K(\phi - 1), \quad (26)$$

$$\left.\frac{\partial \phi}{\partial X}\right|_{X=f_i(Y)} \frac{1}{\sqrt{1+[f_i'(Y)]^2}} - \left.\frac{\partial \phi}{\partial Y}\right|_{X=f_i(Y)} \frac{f_i'(Y)}{\sqrt{1+[f_i'(Y)]^2}} = -K'\phi, \quad (27)$$

where $f'(Y)$ and $f_i'(Y)$ are the derivatives of $f(Y)$ and $f_i(Y)$, respectively. Equations (26) and (27) are deduced from Eq.(1).

It has been deduced in Ref.[16] that the dimensionless crystal growth rate in the X-direction is given by

$$V_{\mathrm{cg},X} = -\eta \frac{Pr}{Sc}\left[\left.\frac{\partial\phi}{\partial X}\right|_{X=f(Y)} - f'(Y)\left.\frac{\partial\phi}{\partial Y}\right|_{X=f(Y)}\right], \tag{28}$$

where η is given by

$$\eta = \frac{c_i - c_s}{\rho_c}, \tag{29}$$

with ρ_c being the density of the growing crystal. In Ref.[18], it is deduced that the dimensionless dissolution rate in the X-direction is given by

$$V_{\mathrm{sd},X} = -\eta' \frac{Pr}{Sc}\left[\left.\frac{\partial\phi}{\partial X}\right|_{X=f_i(Y)} - f_i'(Y)\left.\frac{\partial\phi}{\partial Y}\right|_{X=f_i(Y)}\right], \tag{30}$$

where η' is given by

$$\eta' = \frac{c_i - c_s}{\rho_c'}, \tag{31}$$

with ρ_c' being the density of the source crystal.

4. Transformation of coordinates

The above equations of motion and boundary conditions are transformed into those in terms of general (non-orthogonal) curvilinear coordinates (X_1, Y_1), So, the curved mesh is transformed into a square mesh (see Fig.2 of Ref.[18]). It is convenient to carry out the computation in terms of the coordinates (X_1, Y_1). The transformation of coordinates is done by using the following equations:

$$Y_1 = Y, \qquad X_1 = \frac{X - f(Y)}{f_i(Y) - f(Y)}. \tag{32}$$

Thus, the set of partial differential equations (4)–(7) is transformed into

$$\begin{aligned}
&\frac{1+[f'(Y_1)(1-X_1)+f_i'(Y_1)X_1]^2}{f_i(Y_1)-f(Y_1)}\frac{\partial^2\Xi}{\partial X_1^2} - 2[f'(Y_1)(1-X_1)+f_i'(Y_1)X_1]\frac{\partial^2\Xi}{\partial X_1\partial Y_1} + [f_i(Y_1)-f(Y_1)]\frac{\partial^2\Xi}{\partial Y_1^2}\\
&- \frac{\{[f''(Y_1)(1-X_1)+f_i''(Y_1)\,X_1][f_i(Y_1)-f(Y_1)] - 2[f'(Y_1)(1-X_1)+f_i'(Y_1)X_1][f_i'(Y_1)-f'(Y_1)]\}}{f_i(Y_1)-f(Y_1)}\frac{\partial\Xi}{\partial X_1}\\
&= \frac{1}{Pr}\left(\frac{\partial\Psi}{\partial Y_1}\frac{\partial\Xi}{\partial X_1} - \frac{\partial\Psi}{\partial X_1}\frac{\partial\Xi}{\partial Y_1}\right) - Ra\frac{\partial\theta}{\partial X_1},
\end{aligned} \tag{33}$$

$$\begin{aligned}
&\frac{1+[f'(Y_1)(1-X_1)+f_i'(Y_1)X_1]^2}{f_i(Y_1)-f(Y_1)}\frac{\partial^2\theta}{\partial X_1^2} - 2[f'(Y_1)(1-X_1)+f_i'(Y_1)X_1]\frac{\partial^2\theta}{\partial X_1\partial Y_1} + [f_i(Y_1)-f(Y_1)]\frac{\partial^2\theta}{\partial Y_1^2}\\
&- \frac{\{[f''(Y_1)(1-X_1)+f_i''(Y_1)\,X_1][f_i(Y_1)-f(Y_1)] - 2[f'(Y_1)(1-X_1)+f_i'(Y_1)X_1][f_i'(Y_1)-f'(Y_1)]\}}{f_i(Y_1)-f(Y_1)}\frac{\partial\theta}{\partial X_1}\\
&= \frac{\partial\Psi}{\partial Y_1}\frac{\partial\theta}{\partial X_1} - \frac{\partial\Psi}{\partial X_1}\frac{\partial\theta}{\partial Y_1},
\end{aligned} \tag{34}$$

$$\begin{aligned}
&\frac{1+[f'(Y_1)(1-X_1)+f_i'(Y_1)X_1]^2}{f_i(Y_1)-f(Y_1)}\frac{\partial^2\Psi}{\partial X_1^2} - 2[f'(Y_1)(1-X_1)+f_i'(Y_1)X_1]\frac{\partial^2\Psi}{\partial X_1\partial Y_1} + [f_i(Y_1)-f(Y_1)]\frac{\partial^2\Psi}{\partial Y_1^2}\\
&- \frac{\{[f''(Y_1)(1-X_1)+f_i''(Y_1)\,X_1][f_i(Y_1)-f(Y_1)] - 2[f'(Y_1)(1-X_1)+f_i'(Y_1)X_1][f_i'(Y_1)-f'(Y_1)]\}}{f_i(Y_1)-f(Y_1)}\frac{\partial\Psi}{\partial X_1}\\
&= [f_i(Y_1)-f(Y_1)]\Xi,
\end{aligned} \tag{35}$$

$$\begin{aligned}
&\frac{1+[f'(Y_1)(1-X_1)+f_i'(Y_1)X_1]^2}{f_i(Y_1)-f(Y_1)}\frac{\partial^2\phi}{\partial X_1^2} - 2[f'(Y_1)(1-X_1)+f_i'(Y_1)X_1]\frac{\partial^2\phi}{\partial X_1\partial Y_1} + [f_i(Y_1)-f(Y_1)]\frac{\partial^2\phi}{\partial Y_1^2}\\
&- \frac{\{[f''(Y_1)(1-X_1)+f_i''(Y_1)\,X_1][f_i(Y_1)-f(Y_1)] - 2[f'(Y_1)(1-X_1)+f_i'(Y_1)X_1][f_i'(Y_1)-f'(Y_1)]\}}{f_i(Y_1)-f(Y_1)}\frac{\partial\phi}{\partial X_1}\\
&= \frac{Sc}{Pr}\left(\frac{\partial\Psi}{\partial Y_1}\frac{\partial\phi}{\partial X_1} - \frac{\partial\Psi}{\partial X_1}\frac{\partial\phi}{\partial Y_1}\right),
\end{aligned} \tag{36}$$

where $f'(Y_1)$, $f_i'(Y_1)$ are the derivatives of $f(Y_1)$, $f_i(Y_1)$ and $f''(Y_1)$, $f_i''(Y_1)$ are the second-order derivatives of

$f(Y_1)$, $f_i(Y_1)$, respectively. The boundary conditions of Eqs.(20)–(27) are transformed into

$$\left.\frac{\partial \Psi(X_1,Y_1)}{\partial X_1}\right|_{X_1=0} = \left.\frac{\partial \Psi(X_1,Y_1)}{\partial X_1}\right|_{X_1=1} = \frac{\partial \Psi(X_1,0)}{\partial X_1} = \frac{\partial \Psi(X_1,\lambda)}{\partial X_1} = 0, \tag{37}$$

$$\left.\frac{\partial \Psi(X_1,Y_1)}{\partial Y_1}\right|_{Y_1=0} = \left.\frac{\partial \Psi(X_1,Y_1)}{\partial Y_1}\right|_{Y_1=\lambda} = 0, \tag{38}$$

$$\frac{\partial \Psi(0,Y_1)}{\partial Y_1} - \frac{f'(Y_1)}{f_i(Y_1)-f(Y_1)}\left.\frac{\partial \Psi(X_1,Y_1)}{\partial X_1}\right|_{X_1=0} = 0, \tag{39}$$

$$\frac{\partial \Psi(1,Y_1)}{\partial Y_1} - \frac{f_i'(Y_1)}{f_i(Y_1)-f(Y_1)}\left.\frac{\partial \Psi(X_1,Y_1)}{\partial X_1}\right|_{X_1=1} = 0, \tag{40}$$

$$\Psi(0,Y_1) = \Psi(1,Y_1) = \Psi(X_1,0) = \Psi(X_1,\lambda) = 0, \tag{41}$$

$$\theta(0,Y_1) = 1, \qquad \theta(1,Y_1) = 0, \tag{42}$$

$$\theta(X_1,0) = \theta(X_1,\lambda) = 1 - X_1, \tag{43}$$

$$\left.\frac{\partial \phi(X_1,Y_1)}{\partial Y_1}\right|_{Y_1=0} - [f'(Y_1)(1-X_1) + f_i'(Y_1)X_1]\frac{\partial \phi(X_1,0)}{\partial X_1} = 0, \tag{44}$$

$$\left.\frac{\partial \phi(X_1,Y_1)}{\partial Y_1}\right|_{Y_1=\lambda} - \frac{f'(Y_1)(1-X_1)+f_i'(Y_1)X_1}{f_i(\lambda)-f(\lambda)}\frac{\partial \phi(X_1,\lambda)}{\partial X_1} = 0, \tag{45}$$

$$\left.\frac{\sqrt{1+[f'(Y_1)]^2}}{f_i(Y_1)-f(Y_1)}\frac{\partial \phi(X_1,Y_1)}{\partial X_1}\right|_{X_1=0} - \frac{f'(Y_1)}{\sqrt{1+[f'(Y_1)]^2}}\frac{\partial \phi(0,Y_1)}{\partial Y_1} = K(\phi-1), \tag{46}$$

$$\left.\frac{\sqrt{1+[f_i'(Y_1)]^2}}{f_i(Y_1)-f(Y_1)}\frac{\partial \phi(X_1,Y_1)}{\partial X_1}\right|_{X_1=1} - \frac{f_i'(Y_1)}{\sqrt{1+[f_i'(Y_1)]^2}}\frac{\partial \phi(1,Y_1)}{\partial Y_1} = -K'\phi. \tag{47}$$

5. Computation

Firstly, the crystal growth rate and dissolution rate in the X-direction are calculated in the case of inclined planes of crystal growth face and dissolution face which are expressed by two straight lines,

$$X = f(Y) = Y\tan\alpha_1 \tag{48}$$

and

$$X = f_i(Y) = 1 + Y\tan\alpha_2, \tag{49}$$

respectively. The angle α_1 is the angle made between the line $X = f(Y)$ with Y-axis; and α_2 is the angle made by the line $X = f_i(Y)$ with X =1. The angles α_1 and α_2 may be positive or negative. When the upper part of line $X = f(Y)$ (or $X = f_i(Y)$) inclines forward or backward, the angle α_1(or α_2) is positive or negative, respectively.

After the transformation of coordinates, the partial differential equations (33)–(36) with the boundary conditions of Eqs.(37)–(47) are reduced to a large set of difference equations, and the numerical solutions to the equations are computed using an iteration method with relaxation parameters.[21] In computation, the parameters are taken as follows: Ra=5×10^5, Pr=6, Sc=100, λ=0.2. After the steady-state solutions of θ, ϕ, Ψ, and Ξ are obtained, the function $\phi(X_1, Y_1)$ will be transformed back into $\phi(X,Y)$ in terms of Cartesian coordinates. Then, $V_{\mathrm{cg},X}(Y)$ and $V_{\mathrm{sd},X}(Y)$, the dimensionless crystal growth rates and dissolution rates in the X-direction at various points of the growing crystal face $X = f(Y)$ and the dissolution face $X = f_i(Y)$, will be calculated by using Eqs.(28) and (30), respectively.

Secondly, the stable shapes of the growing crystal face and dissolution face can be calculated as follows. Two suitable planes ($X = f_0(Y) = Y\tan\alpha_1$ and $X = f_{i0}(Y) = 1 + Y\tan\alpha_2$) in which the dimensionless crystal growth rate and dissolution rate in the X-direction at $Y = \lambda$ are equal to those at $Y = 0$ are taken as the initial shapes of growing crystal face and dissolution face, respectively. Then, the face shapes are amended as follows. The crystal growth face is dented or projected a little at the points where $V_{\mathrm{cg},X}(Y)$ is larger or smaller than $V_{\mathrm{cg},X}(0)$, respectively. In the computing program, a curve $X = f_1(Y)$ is substituted for $X = f_0(Y)$, and $f_1(Y)$ is given by

$$f_1(Y) = f_0(Y) - [V_{\mathrm{cg},X}(Y) - V_{\mathrm{cg},X}(0)]_0\Delta t, \tag{50}$$

where Δt is a small increment of dimensionless time. At the same time, the dissolution face is similarly

amended. In the computing program, a curve $X = f_{i1}(Y)$ is substituted for $X = f_{i0}(Y)$, and $f_{i1}(Y)$ is given by

$$f_{i1}(Y) = f_{i0}(Y) - [V_{\mathrm{sd},X}(\lambda) - V_{\mathrm{sd},X}(Y)]_0 \Delta t', \quad (51)$$

where $\Delta t'$ is also a small increment of dimensionless time. In the second step, what we computed are the numerical solutions to Eqs.(33)–(36) under the boundary conditions of Eqs.(37)–(47) in terms of the coordinates (X_1, Y_1). In computation, the growing crystal face and dissolution face are taken to be $X = f_1(Y)$ and $X = f_{i1}(Y)$, instead of $X = f_0(Y)$ and $X = f_{i0}(Y)$, respectively. After the steady-state solutions of θ, ϕ, Ψ and Ξ are obtained, the function $\phi(X_1, Y_1)$ will be transformed into a function in terms of Cartesian coordinates (X, Y), and the $V_{\mathrm{cg},X}(Y)$ at various points of the growing crystal face $X = f_1(Y)$ and the $V_{\mathrm{sd},X}(Y)$ at various points of the dissolution face $X = f_{i1}(Y)$ will be calculated using Eqs.(28) and (30), respectively. Then, the curves $X = f_2(Y)$ and $X = f_{i2}(Y)$ are substituted for $X = f_1(Y)$ and $X = f_{i1}(Y)$, where $f_2(Y)$ and $f_{i2}(Y)$ are given by

$$f_2(Y) = f_1(Y) - [V_{\mathrm{cg},X}(Y) - V_{\mathrm{cg},X}(0)]_1 \Delta t \quad (52)$$

and

$$f_{i2}(Y) = f_{i1}(Y) - [V_{\mathrm{sd},X}(\lambda) - V_{\mathrm{sd},X}(Y)]_1 \Delta t', \quad (53)$$

respectively.

The computation will be carried out as described above—in the nth step, $X = f_n(Y)$ and $X = f_{in}(Y)$ are substituted for $X = f_{n-1}(Y)$ and $X = f_{i(n-1)}(Y)$, where $f_n(Y)$ and $f_{in}(Y)$ are given by

$$f_n(Y) = f_{n-1}(Y) - [V_{\mathrm{cg},X}(Y) - V_{\mathrm{cg},X}(0)]_{n-1} \Delta t, \quad (n = 1, 2, 3, \ldots) \quad (54)$$

and

$$f_{in}(Y) = f_{i(n-1)}(Y) - [V_{\mathrm{sd},X}(\lambda) - V_{\mathrm{sd},X}(Y)]_{n-1} \Delta t', \quad (n = 1, 2, 3, \ldots) \quad (55)$$

respectively. Here the subscript n-1 for the square brackets means that the dimensionless crystal growth rates and dissolution rates in the X-direction, $V_{\mathrm{cg},X}(Y)$ and $V_{\mathrm{sd},X}(Y)$ are calculated for $X = f_{n-1}(Y)$ and $X = f_{i(n-1)}(Y)$, respectively—until the $V_{\mathrm{cg},X}(Y)$ and $V_{\mathrm{sd},X}(Y)$ become constant. When $V_{\mathrm{cg},X}(Y)$ =constant and $V_{\mathrm{sd},X}(Y)$ =constant, the shapes of growing crystal face and dissolution face will not change at all and stable shapes are obtained.

6. Effects of interface kinetics

In computation for the case of inclined planes of the growing crystal face and dissolution face expressed by Eqs.(48) and (49), the parameters are taken as follows: $Ra = 5 \times 10^5$, $Pr = 6$, $Sc = 100$, $K = 500$, K'=2500,[10] or $K = 400$, $K' = 2000$. The case described in Ref.[18] (the interface kinetics was not taken into account) is actually a special case of $K \to \infty$ and $K' \to \infty$.[20]

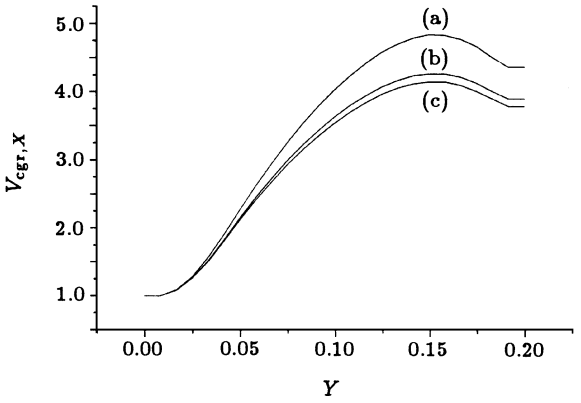


Fig.2. Curves of $V_{\mathrm{cgr},X}$–Y for $\alpha_1 = \alpha_2 = 0$, under the condition: $Ra = 5 \times 10^5$, $Pr = 6$, Sc=100, λ=0.2; (a) without taking the interface kinetics into account; (b) taking the interface kinetics into account, with $K = 500$, K'=2000; (c) same as (b) with K=400, K'=2000.

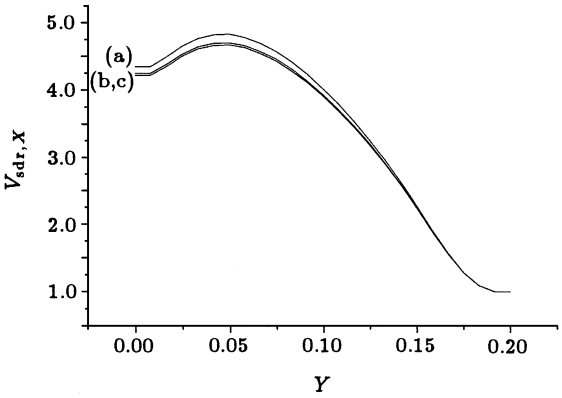


Fig.3. Curves of $V_{\mathrm{sdr},X}$–Y for $\alpha_1 = \alpha_2 = 0$, under the same conditions as in Fig.2.

The calculation results are shown in Figs.2–4. Figure 2 is a plot of the relative crystal growth rate in the X-direction, $V_{\mathrm{cgr},X}$ versus Y for the case of $\alpha_1 = \alpha_2 = 0$. The $V_{\mathrm{cgr},X}(Y)$ is given by

$$V_{\mathrm{cgr},X}(Y) = V_{\mathrm{cg},X}(Y)/V_{\mathrm{cg},X}(0). \quad (56)$$

It can be seen from Fig.2 that the crystal growth rate in the X-direction at the upper part of the growing crystal face is faster than that at the lower part

of the face and the difference between $V_{\mathrm{cgr},X}(\lambda)$ and $V_{\mathrm{cgr},X}(0)$ decreases with K, that is to say, the difference is reduced by taking the interface kinetics into account. We have also calculated $V_{\mathrm{cgr},X}(Y)$ for $\alpha_1 > 0$. The calculation results are similar to those of Refs.[16.18]. It follows that $V_{\mathrm{cgr},X}(Y)$ increases with Y for $\alpha_1 \geq 0$ in general, and the larger the inclination angle α_1, the greater the increase of $V_{\mathrm{cgr},X}$. This means that when the crystal starts growing from the plane face of $X = 0$, the upper part of the growing crystal face is going to incline forward and the inclination gets greater and greater.[16.18]

Figure 3 shows the curves of the relative dissolution rate in the X-direction, $V_{\mathrm{sdr},X}$ versus Y for $\alpha_1 = \alpha_2 = 0$. The $V_{\mathrm{sdr},X}(Y)$ is given by

$$V_{\mathrm{sdr},X}(Y) = V_{\mathrm{sd},X}(Y)/V_{\mathrm{sd},X}(\lambda). \qquad (57)$$

It is seen from Fig.3 that the dissolution rate in the X-direction at the upper part of the dissolution face is slower than that at the lower part of the face and the difference between $V_{\mathrm{sdr},X}(0)$ and $V_{\mathrm{sdr},X}(\lambda)$ decreases slightly with K'.

Figure 4 shows the curves of $V_{\mathrm{cgr},X}$ versus Y for the case of $\tan\alpha_1 = \tan\alpha_2 = -0.3$. It is known from Fig.4 that $V_{\mathrm{cgr},X}(0) \approx V_{\mathrm{cgr},X}(\lambda)$ and the maximum of $V_{\mathrm{cgr},X}(Y)$ decreases with K: namely, it is reduced by taking the interface kinetics into account. The difference between the curves of $V_{\mathrm{sdr},X}(Y)$ versus Y for $\tan\alpha_1 = \tan\alpha_2 = -0.3$ with and without taking the interface kinetics into account is slight; $V_{\mathrm{cgr},X}(0) \approx V_{\mathrm{cgr},X}(\lambda)$ and the maximum of $V_{\mathrm{sdr},X}(Y)$ decreases slightly with K'. Therefore, the curves of $V_{\mathrm{sdr},X}(Y)$ are not shown here.

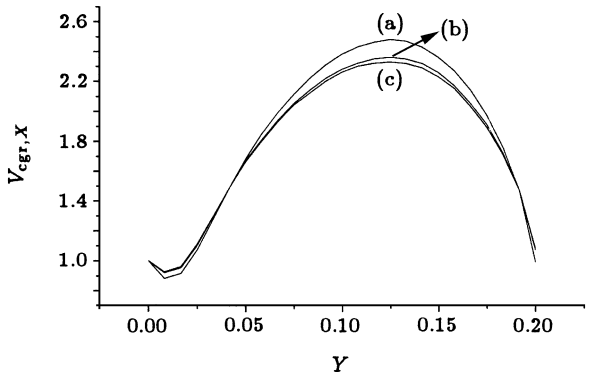


Fig.4. Curves of $V_{\mathrm{cgr},X}$–Y for $\tan\alpha_1 = \tan\alpha_2 = -0.3$ under the same conditions as in Fig.2.

The above-mentioned results are understandable because k is the linear interface kinetics coefficient for crystallization and k' is that for dissolution; K' is five times as large as K; the larger the k and k', the faster the crystal growth rate and the dissolution rate, respectively. When the interface kinetics is not taken into account, the case corresponds to that of $K \to \infty$ and $K' \to \infty$.

It can be easily expected[16.18] from those results that the stable shapes of the growing crystal faces and dissolution faces are suitably shaped curves with their upper parts inclined backward properly no matter whether the interface kinetics is taken into account or not. In addition, the inclination degree of the stable crystal growth face will decrease with K and that of stable dissolution face will decrease slightly with K': namely, the inclination of the stable crystal growth face will be reduced and that of stable dissolution face will be reduced only slightly, by taking the interface kinetics into account.

Those expectations are verified by the calculation of the stable shapes of the growing crystal faces and dissolution faces as shown in Fig.5 which shows how the stable shapes of the growing crystal faces and dissolution faces depend on the interface kinetics and the linear interface kinetics coefficients. This implies that the faster the crystal growth rate and the dissolution rate, the more backward inclined the upper parts of the stable growing crystal faces and dissolution faces.

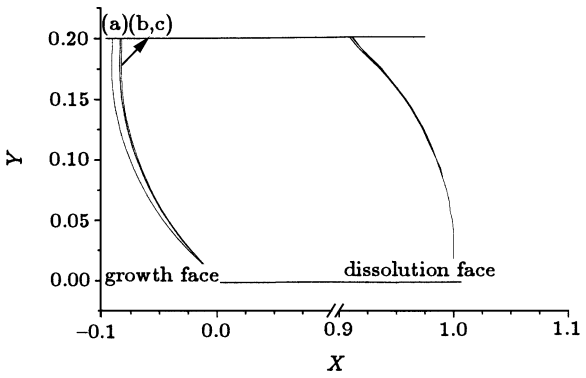


Fig.5. Stable shapes of the growing crystal face and dissolution face under the same conditions as in Fig.2.

The dependence of the stable shapes of the growing crystal faces and dissolution faces on the values of Ra, Sc and Pr bears a similar tendency to that in the case without taking the interface kinetics into account.[16,18] Figure 6 shows how the stable shapes of the growing crystal faces and dissolution faces depend on the value of Ra.

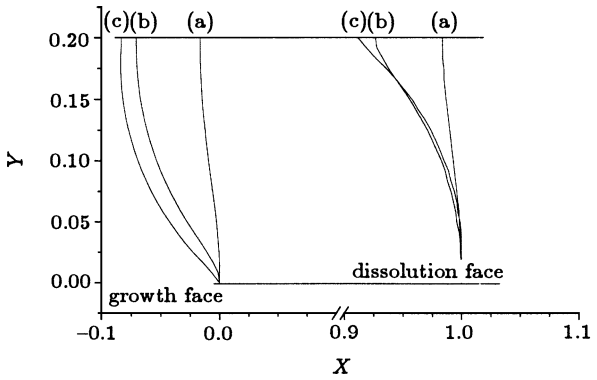


Fig.6. Stable shapes of the growing crystal face and dissolution face under the conditions: $Pr = 6$, $Sc = 100$, $\lambda = 0.2$, $K = 500$, $K' = 2500$, and (a) $Ra = 5 \times 10^3$; (b) $Ra = 5 \times 10^4$; (c) $Ra = 5 \times 10^5$.

7. Effects of anisotropy

Suppose that $X = 0$ and $X = 1$ are two crystal planes with certain indices (such as (100) etc) of the seed crystal and the source crystal, respectively. The crystal growth rate and the dissolution rate along the X-direction are of certain values, so that $K = K_0$ and $K' = K'_0$ when the crystal growth face and dissolution face are the planes of $X = 0$ and $X = 1$, respectively.

When the seed crystal grows and the source crystal dissolves in the normal direction of another crystal plane (such as (110) etc) which is deflected from the above crystal plane (such as (100) etc) (the planes of $X = 0$ and $X = 1$) by an angle θ_0 (such as 45° etc), the crystal growth rate and the dissolution rate are different from the above rates. Now, suppose that $K = K_1$ and $K' = K'_1$. Let

$$\frac{K_1}{K_0} = \frac{K'_1}{K'_0} = \cos^\gamma \theta_0. \tag{58}$$

It is further supposed that

$$K = K_0 \cos^\gamma \theta \tag{59}$$

and

$$K' = K'_0 \cos^\gamma \theta_i, \tag{60}$$

when the seed crystal grows and the source crystal dissolves in directions which deviate from the X-direction by an angle $\theta (0 \le \theta \le \theta_0)$ and $\theta_i (0 \le \theta_i \le \theta_0)$, respectively.

In computation of the stable shapes of the growing crystal faces and dissolution faces, Eqs.(59) and (60) are substituted into Eqs.(46) and (47), respectively, where

$$\tan\theta = f'(Y_1) \tag{61}$$

and

$$\tan\theta_i = f'_i(Y_1), \tag{62}$$

because the seed crystal grows and the source crystal dissolves in normal directions of the growing crystal face and dissolution face, respectively, when they are curved surfaces. In computation, the parameters are taken as follows: $Ra = 5 \times 10^5$, $Pr = 6$, $Sc = 100$, $\lambda = 0.2$, $K_0 = 500$, $K'_0 = 2500$ and $\gamma = -2, 0, 2$ or 4 ($\gamma = 0$ implies that the crystal grows and dissolves isotropically: that is, the anisotropy of crystal growth and dissolution is not taken into account).

The results of the computation are shown in Fig.7. It can be seen that the anisotropy of crystal growth and dissolution may make the inclination of stable growing crystal face smaller or larger, and that of stable dissolution face slightly smaller or larger; to be more exact, the inclination of the stable growing crystal face increases with the value of γ, while that of the stable dissolution face increases only slightly.

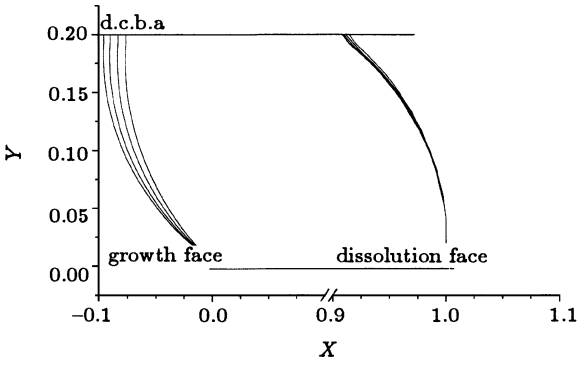


Fig.7. Stable shapes of the growing crystal face and dissolution face under the conditions: $Ra = 5 \times 10^5$, Pr=6, Sc=100, $\lambda = 0.2$, with the anisotropy of crystal growth and dissolution taken into account, $K_0 = 500$, $K'_0 = 2500$, and (a) $\gamma = -2$, (b) $\gamma = 0$, (c) $\gamma = 2$, (d) $\gamma = 4$.

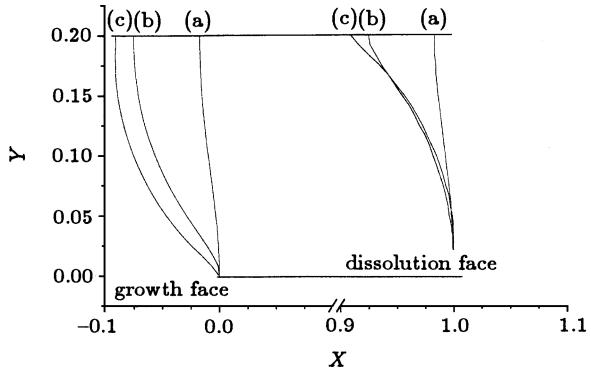


Fig.8. Stable shapes of the growing crystal face and dissolution face under the conditions: Pr=6, Sc=100, λ=0.2, K_0=500, K'_0=2500, γ=2, and (a) $Ra = 5 \times 10^3$; (b) $Ra = 5 \times 10^4$; (c) $Ra = 5 \times 10^5$.

The dependence of the stable shapes of crystal growth faces and dissolution faces on the values of Ra, Sc and Pr shows similar variation to that in the case that the interface kinetics and the anisotropy of crystallization and dissolution are not taken into account.[16,18] Figures 8–10 illustrate how the stable shapes of the growing crystal faces and dissolution faces change with the values of Ra, Sc and Pr, respectively. It can be seen from these figures that the inclination of the stable growing crystal face and dissolution face increase with the increase of Ra or Sc, or with the decrease of Pr. The reason for these results has been stated in Ref.[16]. The increase of Ra or Sc, or the decrease of Pr makes the convection relative to the diffusion in solution stronger. It follows that the stronger the convection relative to the diffusion in solution, the more backward the upper parts of the stable crystal growth face and dissolution face are inclined.

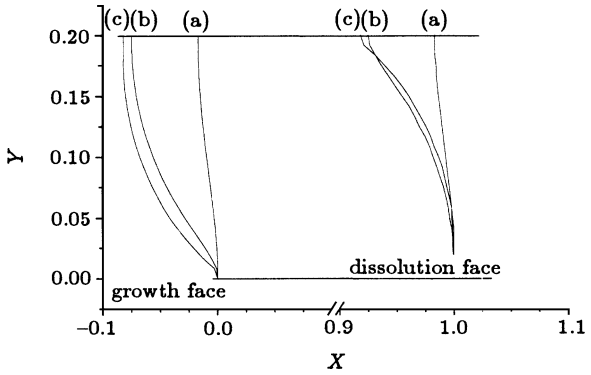


Fig.9. Stable shapes of the growing crystal face and dissolution face under the conditions: $Ra = 5 \times 10^4$, $Pr = 6$, $\lambda = 0.2$, $K_0 = 500$, $K_0' = 2500$, $\gamma = 2$, and (a) $Sc = 10$; (b) $Sc = 100$; (c) $Sc = 1000$.

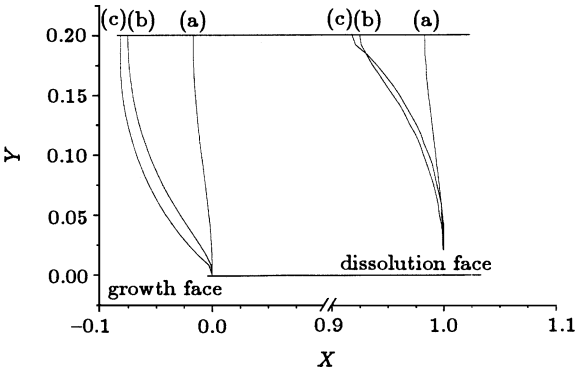


Fig.10. Stable shapes of the growing crystal face and dissolution face under the conditions: $Ra = 5 \times 10^4$, $Sc = 100$, $\lambda = 0.2$, $K_0 = 500$, $K_0' = 2500$, $\gamma = 2$, and (a) $Pr = 60$; (b) $Pr = 6$; (c) $Pr = 0.6$.

8. Conclusion

In conclusion, the stable shapes of crystal growth faces and dissolution faces do exist in the model employed here, which are curves of suitably shaped with their upper parts inclined backward properly no matter whether the interface kinetics and the anisotropy of crystallization and dissolution are taken into account or not.

The interface kinetics will make the inclination degree of the stable crystal growth face reduce and that of stable dissolution face reduce slightly. In addition, the inclination degree of the former decreases with K and that of the latter decreases slightly with K'. In other words, the faster the crystal growth rate and dissolution rate, the more backward inclined the upper parts of the stable crystal growth faces and dissolution faces.

The anisotropy of crystal growth and dissolution may make the inclination of the stable growing crystal face smaller or larger, and that of stable dissolution face only slightly smaller or larger; to be more exact, with the increase of γ, the inclination of the former increases obviously, and that of the latter increases only slightly.

The stable shapes of the growing crystal faces and dissolution faces will change for different values of parameters Ra, Sc and Pr. The stronger the convection relative to the diffusion in the solution, the more backward inclined the upper parts of the stable crystal growth faces and dissolution faces.

References

[1] Huo C R, Ge P W, Xu Z Y and Zhu Z H 1991 *J. Crystal Growth* **114** 486

[2] Huo C R, Ge P W, Xu Z Y and Zhu Z H 1992 *Commun. Theor. Phys.* **17** 135

[3] Xu Z Y, Huo C R, Ge P W and Zhu Z H 1992 *J. Crystal Growth* **125** 365

[4] Zhu Z H 1992 *Journal of the Central Institute for Nationalities (Natural Sciences Edition)* **1** 35

[5] Xu Z Y, Huo C R, Ge P W and Zhu Z H 1993 *J. Crystal Growth* **129** 506

[6] Xu Z Y, Huo C R, Ge P W and Zhu Z H 1994 *J. Crystal Growth* **137** 538

[7] Xu Z Y, Huo C R, Ge P W and Zhu Z H 1994 *Microgravity Sci. Technol.* **VII/2** 124

[8] Xu Z Y, Huo C R, Ge P W and Zhu Z H 1995 *Commun. Theor. Phys.* **24** 159

[9] Huo C R, Xu Z Y, Huang W D, Ge P W and Zhu Z H 1996 *J. Crystal Growth* **158** 359

[10] Zhu Z H, Ge P W, Xu Z Y and Huo C R 1998 *Commun. Theor. Phys.* **30** 391

[11] Zhu Z H, Ge P W, Xu Z Y and Huo C R 1998 *Acta Phys. Sin.* (*Overseas Edition*) **7** 801

[12] Zhu Z H, Ge P W and Xu Z Y 2000 *Chin. Phys.* **9** 321

[13] Baird J K, Meehan E J, Xidis A L and Howard S B 1986 *J. Crystal Growth* **76** 694

[14] Lin H, Rosenberger F, Alexander J I D and Nadarajah A 1995 *J. Crystal Growth* **151** 153

[15] Huo C R, Zhu Z H, Ge P W and Dong C 2001 *Acta Phys. Sin.* **50** 377 (in Chinese)

[16] Zhu Z H, Ge P W, Huo C R, Chen D and Li C R 2001 *J. Crystal Growth* **224** 155

[17] Nagashima K and Furukawa Y 2000 *J. Crystal Growth* **209** 167

[18] Zhu Z H, Luo L, Li C R and Ge P W 2002 *Commun. Theor. Phys.* **37** 117

[19] Mullin J W 1993 *Crystallization* 3rd edn (London, Butterworths)

[20] Wang W and Hu W R 1996 *J. Crystal Growth* **160** 398

[21] Koomin S E 1986 *Computational Physics* Benjamin, Cummings